Master 2ème année **2016-2017**
Thierry.Dauxois@ens-lyon.fr

Exam of the lecture "Physics of Long-Range Interacting Systems"

Friday 24 March 2017

13h30-16h00 : Handwritten lecture notes allowed

1 Question de cours

1(a) Draw and discuss the phase diagram of the BEG model.

1(b) Draw and discuss the phase diagram of self-gravitating particles bounded in a sphere of radius R. Discuss similarities and differences.

1(c) Discuss similarities and differences for what concern the statistical mechanics of 2D vortices and stellar systems.

2 Synchronisation par couplage global

Nous souhaitons étudier la synchronisation d'un grand nombre d'oscillateurs qui interagissent tous, les uns avec les autres. On parle de couplage global.

Nous allons étudier le modèle introduit par Y. Kuramoto en 1984

$$\frac{d\theta_k}{dt} = \omega_k + \varepsilon \frac{1}{N} \sum_l \sin(\theta_l - \theta_k) \ , \qquad k = 1, \ldots, N \ . \tag{1}$$

où θ_k et ω_k sont respectivement la phase et la fréquence propre de l'oscillateur repéré par l'indice k, N le nombre d'oscillateur et ε un nombre réel positif. On introduit le paramètre d'ordre complexe

$$Z = \frac{1}{N} \sum_l \exp\left(i\theta_l\right) = K\, e^{i\Phi}. \tag{2}$$

2(a) Que vaut le module K si les phases sont aléatoires ? Si les phases sont proches ?

2(b) Représenter sur un cercle les deux situations, synchronisée et non synchronisée.

2(c) Réécrire l'équation (1) de manière concise en utilisant le paramètre d'ordre (2).

2(d) Expliquer pourquoi cette équation peut faire croire que les oscillateurs sont découplés. Justifier que ce n'est cependant pas le cas.

2(e) Expliquer pourquoi la phase θ_k est tirée vers la phase moyenne Φ, plutôt que vers la phase d'un oscillateur particulier. Quelle est la quantité qui contrôle la force du couplage ? Expliquer le comportement physique auquel on peut s'attendre ?

2(f) En cherchant des solutions avec le module K constant et la phase Φ en rotation uniforme à la pulsation Ω, déterminer la condition de synchronisation.

2(g) À votre avis, quel est le comportement du paramètre d'ordre si l'on étudie le système à l'aide de simulations numériques ?

3 Gravitation in one dimension

3.1 Introduction

A 1D self-gravitating system consists of N sheets of mass density m uniformly distributed in the y–z plane, free to move along the x axis. The dynamics of the sheets is the same as the dynamics of point particles of mass m interacting by a linear potential. The particles are free to cross one another. The thermodynamic limit, $\lim_{N\to\infty} mN = M =$ constant, is equivalent to the Kac prescription necessary to guarantee the extensivity of the energy.

3.1(a) Denoting $\lambda(x,t)$ the mass density and $\phi(x,t)$ the gravitational potential, gives the Poisson equation.

3.1(b) In order to simplify the expressions, we will work with dimensionless variables. We shall rescale the mass, length, velocity, potential, and energy by M, L_0 (an arbitrary length scale), $V_0 = \sqrt{2\pi GML_0}$, $\phi_0 = 2\pi GML_0$ and $E_0 = MV_0^2 = 2\pi GM^2L_0$, respectively. Considering $G = M = 1$ and defining appropriately a dynamical time scale τ_D, the Poisson equation can be written

$$\nabla^2\phi(x,t) = 2\rho(x,t). \tag{3}$$

Gives the expression of τ_D as a function of the other variables.

3.1(c) For a particle (sheet) of (reduced) mass density located at x', gives the expression of the density.

3.1(d) Deduce the expression of the associated potential.

3.1(e) Is it a long-range or a short-range potential?

3.1(f) Comment the presence or absence of singularities of the potential, in particular with the 3D counter analog.

3.1(g) A system's energy takes into account the total work necessary to bring a particle from infinity (or from a position where the potential is zero) to a position $\mathbf{q}$, i.e. $\int [\phi(\mathbf{q}) - \phi(\infty)]\,\mathrm{d}\mathbf{q}$. What is the difference between the 1D and 3D self-gravitating potential? What is the solution?

3.2 Molecular Dynamics

The reduced Hamiltonian for a system of N particles interacting by a one-dimensional gravitational potential is

$$\mathcal{H}(x,v) = \sum_{i=1}^{N} \frac{v_i^2}{2} + \frac{1}{2N}\sum_{i,j}^{N} |x_i - x_j|, \tag{4}$$

This Hamiltonian, along with Hamilton's equations of motion, completely determines the dynamics of the system.

3.2(a) Gives the acceleration of a particle at position x, due to its interaction with the other particles.

3.2(b) Simplify this expression by introducing $N_>(x)$ and $N_<(x)$ the numbers of particles to the right and to the left of x, respectively.

3.2(c) What is the scaling with N of the direct simulation of this system?

3.2(d) Explain why the simulation may be simplified by using a vector containing the indices of each particle, and reordering it according to each particle's position at each new calculation.

3.2(e) Let us simulate numerically the evolution of a system of particles that are initially distributed uniformly with positions x_i where $x_i \in [-x_m, x_m]$ and velocities $v_i \in [-v_m, v_m]$. Introducing $\eta = (4x_m v_m)^{-1}$, write the initial distribution function $f_0(x, v)$

3.2(f) Compute the initial energy. Hint: Find first the potential that is the solution of the Poisson equation.

3.3 Equilibrium

We are interested in the relaxation of the system to equilibrium.

3.3(a) Justify and criticize the idea to look for a solution as $f_{mb}(x, v) = C\, e^{-\beta(v^2/2+\phi_{eq}(x))}$. Discuss the signification of C and β.

3.3(b) Determine the equation satisfied by the equilibrium potential $\phi_{eq}(x)$.

3.3(c) Solve this equation and show that $\phi_{eq}(x) = -\frac{1}{\beta} \ln\left[\frac{1}{4}\,\mathrm{sech}^2\left(\frac{\beta x}{2}\right)\right]$ where $\mathrm{sech}\, x = 1/\cosh x$.

3.3(d) Derive the distribution function at equilibrium $f_{eq}(x, v)$.

3.3(d) Determine the value of β.

3.3(e) Figure 1 compare the equilibrium distributions with the results of molecular dynamics simulations. Discuss.

3.3(f) Recall in a few lines the main points of the theory proposed by Lynden-Bell to predict the results of molecular dynamics simulations.

3.3(g) Figure 2 compare the predictions of Lynden-Bell statistics with the results of molecular dynamics simulations. Discuss.

3.3(h) Conclude by relying the above findings with the Kac rescaling.

Inspired by *Nonequilibrium statistical mechanics of systems with lon-range interactions* by Y. Levin, R. Pakter, F. B. Rizzato, T. N. Teles, F.P.C Benetti, Physics Reports 535, 1-60 (2014).

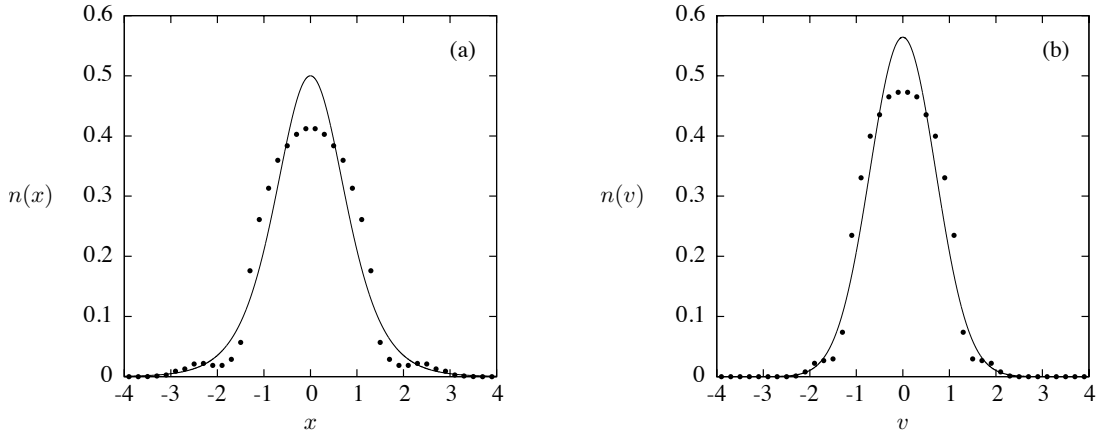

Figure 1: Distributions in (a) position and (b) velocity for a 1D gravitational system with $\mathcal{E}_0 = 0.75$, obtained using MD simulations (points), averaged over times $t = 1000\tau_D$ to $t = 1100\tau_D$, compared with the equilibrium distributions (lines). Repeating the MD simulation for the same initial energy but different initial conditions and taking the average value of the resulting distributions, error bars showing the standard error are smaller than the symbol size.

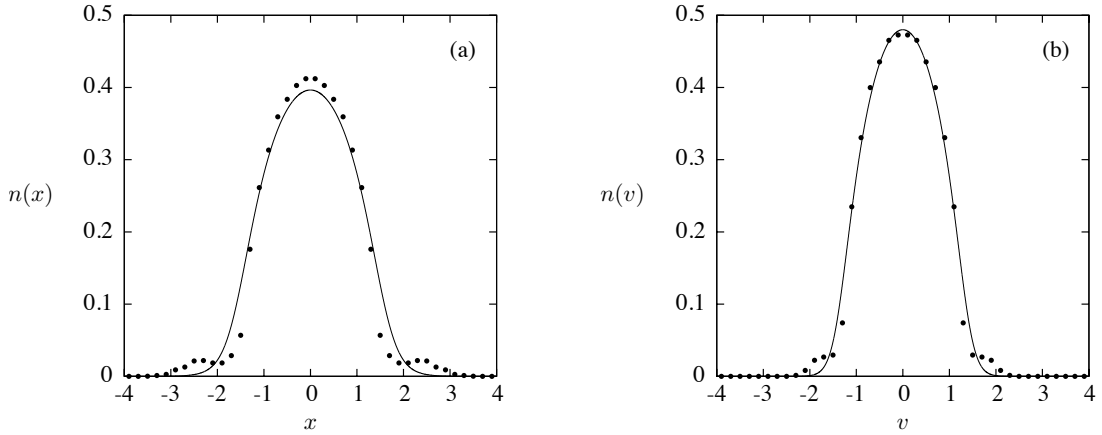

Figure 2: Distributions in (a) position and (b) velocity for a 1D gravitational system with $\mathcal{E}_0 = 0.75$, obtained using MD simulations (points), averaged over $t = 1000\tau_D$ and $t = 1100\tau_D$, compared with the LB distributions (lines). Error bars are smaller than the symbol size.

Correction

1. Question de cours

1(a) Phase diagram for the BEG model.

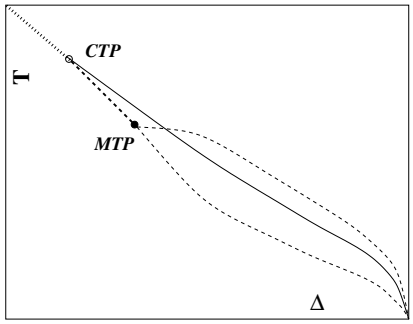

A schematic phase diagram near the canonical tricritical point (CTP) and the microcanonical one (MTP) is given above. In the region between the two tricritical points, the canonical ensemble yields a first order phase transition at a higher temperature, while in the microcanonical ensemble the transition is still continuous. It is in this region that negative specific heat appears. Beyond the microcanonical tricritical point, the temperature has a jump at the transition energy in the microcanonical ensemble. The two lines emerging on the right side from the MTP correspond to the two limiting temperatures which are reached when approaching the transition energy from below and from above. The two microcanonical temperature lines and the canonical first order phase transition line all merge on the $T = 0$ line at $\Delta = 1/2$.

1(b) Phase diagram for self-gravitating systems bounded in a sphere of radius R. For sufficiently low energy or temperature there is no equilibrium state and the system undergoes gravitational collapse.

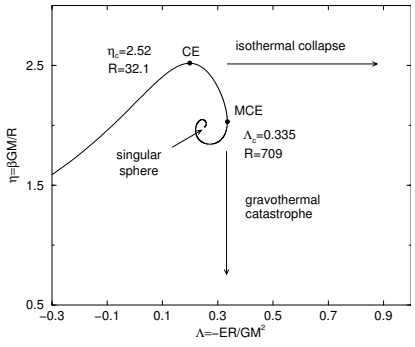

The caloric curve has a striking spiral behavior parametrized by the density contrast $\rho = n(0)/n(R)$ going from 1 (homogeneous system to $+\infty$ (singular sphere) as we proceed along the spiral.

There is no equilibrium state below $E_c = -0.335\mathcal{G}M^2/R$. In that case, the system is expected to collapse indefinitely. This is called *gravothermal catastrophe* in the micro canonical ensemble (fixed E) and *isothermal collapse* in the canonical ensemble (fixed T).

Dynamical models show that the collapse is self-similar and develops a finite time singularity.

In the microcanonical ensemble, the series of equilibria becomes unstable after the point MCE. At that point, solutions pass from local entropy maxima to saddle points.

In the canonical ensemble, the series of equilibria becomes unstable after the point CE. At that point, solutions pass from minima of free energy to saddle points.

Before the point MCE, the curve $T(E)$ is univalued so that the equilibriums states are always stable in the microcanonical ensemble (they are global entropy maxima). By contrast, after the point MCE the $T(E)$ curve is multivalued and this can lead to a first order phase transition in the canonical ensemble. The gaseous and condensed phases are thus connected by a Maxwell plateau which replaces the region of negative specific heats. Point CE is therefore called a canonical tricritical point, while MCE is the microcanonical tricritical point.

It can be noted that the region of negative specific heats between CE and MCE is stable in the microcanonical ensemble but unstable in the canonical ensemble.

1(c) Despite the differences, the statistical mechanics of 2D vortices and stellar systems are relatively similar. Like the point vortex gas, the self-gravitating gas is described at statistical equilibrium by the Boltzmann distribution, and its structure determined by solving a Boltzmann-Poisson equation. In analogy between stellar systems and two dimensional vortices, the star density plays f the role of vorticity ω, the force the role of the velocity and the gravitational potential ϕ the role of the stream function ψ. The crucial point to realize is that, for the two systems, the interaction is long-range unshielded Coulombian interaction (in $d = 3$ or 2 dimensions). This makes the connexion between point vortices and stellar systems deeper than between vortices and electric charges for example.

There are, on the other hand, fundamental differences between star and vortices. A star creates an acceleration while a vortex creates a velocity. The gravitational interaction is attractive and directed along the line joining the particles while the interaction of vortices is rotational and perpendicular to the line joining the vortices.

2. Synchronisation par couplage global

2(a) Si les phases sont aléatoirement réparties sur le cercle unité, $K \simeq 0$, alors que si les phases sont proches $K \simeq 1$.

2(b) Si les phases θ_l sont aléatoires, les phases sont réparties aléatoirement sur le cercle. Au contraire, dans l'état synchronisé toutes les phases sont proches d'un même point.

2(c) En développant le sinus, on obtient

$$\begin{aligned}
\frac{d\theta_k}{dt} &= \omega_k + \varepsilon \frac{1}{N} \sum_l (\sin\theta_l \cos\theta_k - \sin\theta_k \cos\theta_l) && (5)\\
&= \omega_k + \varepsilon \cos\theta_k \left(\frac{1}{N} \sum_l \sin\theta_l \right) - \varepsilon \sin\theta_k \left(\frac{1}{N} \sum_l \cos\theta_l \right) && (6)\\
&= \omega_k + \varepsilon \cos\theta_k X - \varepsilon \sin\theta_k Y && (7)\\
&= \omega_k + \varepsilon \cos\theta_k K \cos\Phi - \varepsilon \sin\theta_k K \sin\Phi && (8)\\
&= \omega_k + \varepsilon K \sin(\theta_k - \Phi). && (9)
\end{aligned}$$

2(d) Cette équation peut effectivement faire croire que les oscillateurs sont découplés. Il n'en est cependant rien, puisque les équations sont couplées à travers le module et la phase du paramètre d'ordre Z. On pourrait envisager d'essayer d'écrire l'équation d'évolution du paramètre d'ordre Z, mais l'équation $\dot{Z} = ...$ ne dépend pas que de Z et n'est donc pas fermée.

2(e) De manière plus spécifique, la phase θ_k est donc tirée vers la phase moyenne Φ, plutôt que vers la phase d'un oscillateur particulier. Par ailleurs, la force de couplage est directement proportionnel à la cohérence K. Cette proportionnalité crée un feedback positif entre le couplage et la cohérence. Lorsque la population devient plus cohérente, K croît et le couplage effectif $K\varepsilon$ augmente, ce qui a tendance) collecter encore plus d'oscillateurs dans le groupe d'oscillateurs synchronisés.

2(f) En prenant donc $\Phi = \Omega t$, l'équation (9) conduit à

$$\frac{d\theta_k}{dt} = \omega_k + \varepsilon K \sin(\theta_k - \Omega t). \tag{10}$$

On est donc ramené à l'équation d'un oscillateur forcé de manière périodique. Il y a donc deux situations possibles.

Si le forçage est suffisant, i.e. $\varepsilon K > |\omega_k - \Omega|$, on est à l'intérieur de la langue d'Arnold, et le système est synchronisé: $\theta_k = \Omega t + \phi_k$, avec $\omega_k + \varepsilon K \sin\phi_k = 0$. Ces oscillateurs seront accrochés sur la fréquence Ω.

Au contraire, les oscillateurs avec $\varepsilon K < |\omega_k - \Omega|$, ne seront pas synchronisés: $\dot{\theta}_k \neq \Omega$. Ils tourneront autour du cercle de manière non uniforme.

Cette explication due à Kuramoto explique donc simplement pourquoi le système se divise en deux groupes.

2(g) Les simulations montrent que pour toute valeur de K inférieure à une valeur critique K_c, les oscillateurs agissent comme s'ils étaient découplés: les phases se distribuent de manière uniforme autour du cercle, et cela à partir de n'importe quelle condition initiale. Par la suite $K(t)$ oscille pour atteindre zéro avec des fluctuations d'ordre $N^{-1/2}$ comme on peut l'attendre.

En revanche, lorsque $K > K_c$, cet état incohérent devient instable et $K(t)$ croît de manière exponentielle du fait de la nucléation d'un petit cluster d'oscillateurs qui se synchronisent. Le module du paramètre d'ordre sature à une valeur $K_\infty < 1$ avec toujours des fluctuations d'ordre $N^{-1/2}$.

La population des oscillateurs se divisent en deux groupes, ceux près du centre de la distribution qui se synchronisent sur la pulsation Ω, alors que ceux près des queues tournent à leur pulsation propre. Plus on augment K, plus le nombre d'oscillateurs synchronisés augmentent.

3 Gravitation in one dimension

3.1. Introduction

3.1(a) The Poisson equation for this system is

$$\nabla^2\phi(x,t) = 4\pi G\lambda(x,t) \tag{11}$$

where G is the gravitational constant and $\lambda(x,t)$ the mass density.

3.1(b) $\tau_D = (4\pi G\rho_0)^{-1/2}$.

3.1(c) $\rho(x, x') = \delta(x - x')$

3.1(d) $\phi(x, x') = |x - x'|$.

3.1(e) The potential is therefore increasing with the distance, and therefore a long-range potential.

3.1(f) A particularly interesting aspect of the one-dimensional gravity is that the interaction potential does not have any singularities, which simplifies significantly molecular dynamics (MD) simulations, allowing us to explore in great detail the relaxation of this model to the qSS.

3.1(g) For 3D self-gravitating systems the potential at infinity is zero, and for plasmas it is zero at the conducting wall. However, it is important to note that for 1D and 2D self-gravitating systems, the potential diverges at infinity. Since this divergent term appears in both the initial and the final state, the problem is avoided by using a renormalized energy. See Ref Teles et al, J. Stat. Mech P05007 (2010) for more details.

3.2. Molecular dynamics

3.2(a) $\ddot{x} = -\frac{1}{N}\sum_{i=1}^{N} \frac{x - x_i}{|x - x_i|}$

3.2(b) $\ddot{x} = \frac{N_>(x) - N_<(x)}{N}$

3.2(c) To simulate the system according to above equation requires time that scales with N^2.

3.2(d) However, the simulation may be simplified by using a vector containing the indices of each particle, and reordering it according to each particle's position at each new calculation. Above equation then may be written as $\ddot{x} = \frac{(N-i)-(i-1)}{N} = \frac{N-2i+1}{N}$, where i is the index of the particle at position x.

This simplification involves no approximation; the advantage is purely computational, for the simulations become more efficient regarding the computational time —the typical time required to order a vector of size N varies at most with $N \ln N$. Using this method, the trajectories may be obtained exactly, that is, at machine precision. However, for the exact procedure, the trajectories must be calculated at each collision, and the number of collisions grows as N^2.

3.2(e) $f_0(x, v) = \eta\Theta(x_m - |x|)\Theta(v_m - |v|)$

3.2(f) The potential that is the solution of the Poisson equation (3) at $t = 0$ is

$$\frac{d^2}{dx^2}\phi(x) = \begin{cases} \frac{1}{x_m} & \text{for } |x| \le x_m \\ 0 & \text{for } |x| \ge x_m \end{cases} \tag{12}$$

with boundary conditions $\lim_{|x|\to\infty} \phi(x) = |x|$ and $\phi'(0) = 0$. The solution is given by

$$\phi(x) = \begin{cases} \frac{x^2}{2x_m} + \frac{x_m}{2} & \text{for } |x| \le x_m \\ |x| & \text{for } |x| \ge x_m. \end{cases} \tag{13}$$

Using the definition of the mean energy $\mathcal{E}_0 = \int (p^2/(2m) + \phi/2) f(q, p) \mathrm{d}p\mathrm{d}q$, the initial energy of the system is found to be $\mathcal{E}_0 = \frac{v_m^2}{6} + \frac{1}{3}$ where without loss of generality we have set $x_m = 1$.

3.3. Equilibrium

3.3(a) $f_{mb}(x,v) = Ce^{-\beta(v^2/2+w(x))}$ is the expected solution in the canonical ensemble, with β the Lagrange multiplier used to conserve total energy, C a normalization constant and $\omega(x)$ the potential of mean force; As $N \to \infty$, interparticle correlations vanish and $\omega(x) \sim \phi(x)$. However, we know that the canonical ensemble is not well defined for a long-range potential: such an ansatz is therefore not totally expected as discussed during the lecture.

3.3(b) If the system relaxes to equilibrium the gravitational potential must satisfy the Poisson equation $\nabla^2\phi(x) = 2n(x)$ where $n(x)$ is the equilibrium density distribution. Using the Maxwell-Boltzmann distribution, $f_{mb}(x,v) = Ce^{-\beta(v^2/2+w(x))}$, the equilibrium density distribution is given by

$$n(x) = \int f_{mb}(x,v)\,\mathrm{d}v = \sqrt{\frac{2\pi}{\beta}} C \mathrm{e}^{-\beta\omega(x)}\,, \tag{14}$$

As $N \to \infty$, interparticle correlations vanish and $\omega(x) \sim \phi(x)$. Substituting equation (14) in the Poisson-Boltzmann equation in its dimensionless form, we get

$$\nabla^2\phi_{eq}(x) = \sqrt{\frac{8\pi}{\beta}}\, C\, e^{-\beta\phi_{eq}(x)}\,. \tag{15}$$

3.3(c) Solving this equation using the boundary conditions $\lim_{|x|\to\infty}\phi_{eq}(x) = |x|$ and $\phi'_{eq}(0) = 0$, the potential is found to be $\phi_{eq}(x) = -\frac{1}{\beta}\ln\left[\frac{1}{4}\operatorname{sech}^2\left(\frac{\beta x}{2}\right)\right]$.

3.3(d) The distribution function is given by $f_{eq}(x,v) = \sqrt{\frac{\beta^3}{32\pi}}\mathrm{e}^{-\frac{\beta v^2}{2}}\operatorname{sech}^2\left[\frac{\beta x}{2}\right]$.

3.3(e) The value of $\beta = 3/(2\mathcal{E})$ is determined by the conservation of energy with $\bar{f}(x,v) = f_{eq}(x,v)$.

3.3(e) The equilibrium density and velocity distributions are given by $n(x) = \frac{\beta}{4}\operatorname{sech}^2\left(\frac{\beta x}{2}\right)$ and $n(v) = \sqrt{\frac{\beta}{2\pi}}e^{-\beta v^2/2}$. As can be seen in Fig 1, the predictions of equilibrium statistical mechanics are very different from those of MD simulations. This clearly shows that the ergodicity required by the Boltzmann-Gibbs statistical mechanics is violated.

3.3(f) The application of Lynden-Bell statistics to one-dimensional gravitational systems has spanned various decades, with divergent results. See lecture for more details.

In order to determine $f_{lb}(x,v)$ for a one-dimensional gravitational system, we need to calculate the gravitational potential $\phi_{lb}(x)$. To do this we must solve the Poisson equation with $f(x,v) = f_{lb}(x,v)$ and the one-particle energy given by $\epsilon(x,v) = v^2/2 + \phi_{lb}(x)$. Integrating the Lynden-Bell distribution over momentum, we obtain the Poisson equation

$$\frac{d^2\phi_{lb}(x)}{dx^2} = -\sqrt{\frac{8\pi}{\beta}}\eta\mathrm{Li}_{1/2}\left[-e^{-\beta(\phi_{lb}(x)-\mu)}\right], \tag{16}$$

where μ is the Lagrange multiplier associated to normalisation of the distribution function, and with boundary conditions $\lim_{|x|\to\infty}\phi_{lb}(x) = |x|$ and $\phi'_{lb}(0) = 0$, where $\mathrm{Li}_n(x)$ is the polylogarithm function of order n. The solution to this equation is obtained numerically.

3.3(g) Fig 2, which compares the position and the velocity distributions $n(x) = \int f_{lb}(x, v)\mathrm{d}v$ and $n(v) = \int f_{lb}(x, v)\mathrm{d}x$ with the results of MD simulations, show that the predictions of LB statistics are better than the equilibrium distribution, although not perfect.

The problem, common to both BG and LB statistics, is that in thermodynamic limit, systems with LR forces are intrinsically non-ergodic, invalidating the basic assumptions that underlie both theories. For systems with a finite number of particles, however, ergodicity is restored on a sufficiently long time scale. Such systems will eventually relax to the BG equilibrium (if it exists, and the BG entropy has a maximum), after being trapped in a qSS for a time proportional to the number of particles in the system.

3.3(h) The Kac scaling required by the long-range nature of the interaction potential destroys the correlations (collisions) between the particles. Therefore, in thermodynamic limit, long-range systems are intrinsically collisionless – particles move under the action of the mean-field potential produced by all the other particles. In general, the mean-field potential has a complex dynamics, characterized by quasi-periodic oscillations. It is possible, therefore, for some particle to enter in resonance with the oscillations and gain large amounts of energy at the expense of the collective motion. This process, known as Landau damping, diminishes the amplitude of the oscillations and leads to the formation of a tenuous halo of highly energetic particles which surround the high density core. After all the oscillations have died out, a stationary state state is established. The phase space distribution of particles in the quasi-stationary state has a characteristic core-halo structure, very different from the predictions of either Boltzmann-Gibbs or Lynden Bell statistics. Once the stationary state is established, there is no longer a mechanism through which highly energetic particles of the halo can equilibrate with the particles of the core, and the ergodicity is broken.